Manuscript for Biochimica et Biophysica Acta (BBA) – Biomembranes (Regular papers)

Oligomerization–function relationship of EGFR on living cells detected by the coiled-coil labeling and FRET microscopy

Hirotaka Yamashita[a], Yoshiaki Yano[a], Kenichi Kawano[a], and Katsumi Matsuzaki[a, *]

[a]Graduate School of Pharmaceutical Sciences, Kyoto University, Sakyo-ku, Kyoto 606-8501, Japan

[*]Correspondence: mkatsumi@pharm.kyoto-u.ac.jp

Telephone: 81-75-753-4521. Fax: 81-75-753-4578.

Keywords

Dimerization / live-cell imaging / FRET

Hilights

•FRET-based analysis revealed oligomeric states of EGFRs on living membranes.

•EGF stimulation dimerized only two-thirds of EGFR monomers.

•Cholesterol and ganglioside had no significant effect on EGFR dimerization.

•EGFR phosphorylation was mainly induced by dimers with two EGFs.

Footnotes

Abbreviations: EGFR, Epidermal Growth Factor Receptor; EGF, Epidermal Growth Factor; FRET, Förster Resonance Energy Transfer; MAPK, mitogen-activated protein kinase

Abstract

The epidermal growth factor receptor (EGFR) is a well-studied receptor tyrosine kinase and an important anticancer therapeutic target. The activity of EGFR autophosphorylation and transphosphorylation, which induces several cell signaling pathways, has been suggested to be related to its oligomeric state. However, the oligomeric states of EGFRs induced by EGF binding and the receptor–ligand stoichiometry required for its activation are still controversial. In the present study, we performed Förster resonance energy transfer (FRET) measurements by combining the coiled-coil tag–probe labeling method and spectral imaging to quantitatively analyze EGFR oligomerization on living CHO-K1 cell membranes at physiological expression levels. In the absence of its ligands, EGFRs mainly existed as monomers with a small fraction of predimers (~10%), whereas ~70% of the EGFRs formed dimers after being stimulated with the ligand EGF. Ligand-induced dimerization was not significantly affected by the perturbation of membrane components (cholesterol or monosialoganglioside GM3). We also investigated both dose- and time- dependences of EGF-dependent EGFR dimerization and autophosphorylation. The formation of dimers occurred within 20 s of the ligand stimulation and preceded its autophosphorylation, which reached a plateau 90 s after the stimulation. The EGF concentration needed to evoke half maximum dimerization (~ 1 nM) was lower than that for half-maximum autophosphorylation (~ 8 nM), which suggested the presence of an inactive dimer binding a single EGF molecule.

1. Introduction

The epidermal growth factor receptor (also called EGFR, ErbB1, or HER1) is one of the most well-studied receptor tyrosine kinases related to cell differentiation, proliferation, and other physiological activities via several signaling pathways, including the MAPK (mitogen-activated protein kinase) pathway [1]. EGFRs are important anticancer therapeutic targets because certain cancer tissues overexpress them, frequently with aberrant mutations [2–4]. The intracellular signaling pathways activated by EGFRs are triggered by homo/heterooligomerization between EGFRs or an EGFR and other ErbB family receptors, which results in the autophosphorylation/transphosphorylation of tyrosine residues at the C terminus of the receptors [5–7]. Previous studies using X-ray crystallography suggested that the extracellular domains of EGFRs may markedly change from a tethered form [8] to a extended form when EGFRs bind to their ligands: epidermal growth factor (EGF) or transforming growth factor-α [9,10]. However, the actual behavior of EGFRs on cell membranes upon ligand binding is more complex than a simple transition from unliganded inactive monomers to liganded active dimers [11–13]. Although the size of EGFR clusters is controversial, it is generally accepted that EGF binding enhances receptor oligomerization, which activates receptors. Several studies reported that some EGFRs could form inactive dimers (predimer), even in the absence of a ligand [14–16]. EGFR dimers, higher-order oligomers, and aggregates have been identified in the activation process [15,17]. Furthermore, there are a number of possibilities for stoichiometry of ligand and receptor that is required for the signaling. One reason for the inconsistency in oligomeric states in the literature is the differences in the experimental conditions such as the host cells used and expression levels of the receptors. For example, the dimer fraction in the absence of ligands can depend on the total concentration of receptors in the membrane because the unoccupied EGFR monomer is generally in equilibrium with the unoccupied EGFR dimer [13]. Another reason for the apparent diversity has been attributed to limitations in the conventional methods used to evaluate the oligomerization of membrane proteins. The solubilization by detergents or fixation of cells has been shown to significantly perturb interprotein interactions in native cell membranes [14,15]. For living cell analyses, energy transfer methods using genetic luminescent/fluorescent proteins sometimes provide controversial findings on the oligomeric states of target proteins because of a limited ability to control the labeling ratio of the energy donor to the acceptor [18].

We here used EGFRs labeled with fluorophores by coiled-coil labeling [19] to clarify the oligomeric states of EGFRs in the activation process. The coiled-coil method utilizes the

formation of a strong and specific noncovalent bond between the E3-peptide $(EIAALEK)_3$ fused to the N-terminus of the target protein and the fluorophore-conjugated K4-peptide $(KIAALKE)_4$ (total size, 5–6 kDa). This small post-translational labeling method can specifically detect cell-surface proteins in living cells. We recently reported that a combination of the coiled-coil labeling method and Förster resonance energy transfer (FRET) measurements by spectral imaging enabled an exact analysis of the oligomeric states of target membrane proteins [20]. In the present study, we examined the relationship between the oligomeric states of EGFRs and their autophosphorylation levels to elucidate the activation mechanism.

2. Materials and methods

2.1. Preparation of K4 probes

The K4 peptide $(KIAALKE)_4$ was synthesized using a standard 9-fluorenylmethyloxycarbonyl-based solid-phase method [19]. Each fluorophore (Alexa Fluor 568, Alexa Fluor 647, Tetramethylrhodamine, or Cy5 (Life Technologies, Carlsbad, CA)) was added to the N-terminus of the K4 peptide on resin by treating the fluorophores with succinimidyl ester derivatives [19]. After the fluorophore-conjugated peptides had been purified by reversed-phase HPLC, their molecular masses were confirmed by MALDI (Matrix-assisted laser desorption/ionization) mass spectroscopy. The concentrations of the K4 probes were determined according to the absorbance of each fluorophore.

2.2. Plasmid construction

A DNA plasmid coding rat EGFR was constructed based on pcDNA3 (Life Technologies) by inserting the sequence of the E3-tagged EGFR (signal sequence-E3 tag-linker (ggcggcggcatcgat)-rat EGFR sequence-stop codon) at the multicloning site (see Table A1 in the Supporting Material). Rat EGFR was cloned from the rat brain (see supplemental information). Other pcDNA3-based plasmids containing E3-GpA* (G83I mutant) and E3-M2 were constructed as described previously [20]. A stable Flp-in CHO (Chinese hamster ovary) cell line expressing E3-β_2AR (1.3×10^5 receptors/cell) [21] was used as an expression standard.

2.3. Cell culture

CHO cells, which have only negligible endogenous ErbB family receptors [22–25], were used for the transient expression of membrane proteins. CHO-K1 and Flp-in CHO cells (Life Technologies) stably expressing E3-β_2AR were cultured in Ham's F12 medium supplemented with 10% FBS, L-glutamine, penicillin, and streptomycin at 50 μg/mL at 37°C in a 5% CO_2 incubator.

2.4. Transient transfection

CHO-K1 cells (1.0×10^5 per dish) were seeded in a 35-mm glass bottom dish (Advanced TC treated, Greiner Bio-one, Germany) and a polymer bottom dish for confocal imaging and immunoblotting, respectively. The medium was changed to a serum-free medium after overnight incubation, and the cells were incubated with a transfection mixture composed of 1.0 μg of plasmid DNA, 4.0 μL of Lipofectamine LTX (Life Technologies), and 400 μL of Opti-MEM (Life Technologies) per dish. The medium of the CHO-K1 cells was changed to fresh medium containing 10% FBS 5 h after the transfection. These cells were used in experiments 18 h after the transfection. To eliminate the effects of growth factors included in FBS, E3-EGFR-expressing cells were serum-starved for at least 3 h before being examined.

2.5. Immunoblotting

After the transfection, E3-EGFR expressing cells were incubated with or without rat EGF (Higeta Shoyu, Tokyo, Japan) in PBS(+) (137 mM NaCl, 8.1 mM Na_2HPO_4, 2.68 mM KCl, 1.47 mM KH_2PO_4, 0.9 mM $CaCl_2$, 0.33 mM $MgCl_2$, pH 7.4) for 5 min. After removing PBS, the cells were lysed with 500 μL lysis buffer (1% SDS, 1 mM sodium orthovanadate, 10 mM Tris-HCl (pH 7.4), protease inhibitor cocktail (Nacalai Tesque, Kyoto, Japan)) to stop the phosphorylation reaction. Lysates were boiled for 5 min and centrifuged (21,900g, 5 min). Three μL of each supernatant was dropped on to the PVDF membranes. After drying, the PVDF membranes were treated with the p-EGFR (Tyr1173) antibody (sc-101668, Santa Cruz Biotechnology, Dallas, TX) or EGFR antibody (sc-373746, Santa Cruz). The secondary antibody labeled with horseradish peroxidase (anti-rabbit (sc-2004) or anti-mouse (sc-2005), Santa Cruz) was then added, and immunoreactive species were detected by the ECL reagent (Nacalai Tesque). The phosphorylated-EGFR/total EGFR ratios of chemiluminescence intensities were used as the phosphorylation level. In Western blotting,

20 μL of each lysate was applied to a 7% polyacrylamide gel. After SDS-PAGE, the separated proteins were transferred onto PVDF membranes, which were then treated in the same manner as described above.

2.6. Confocal microscopy

All imaging experiments were performed using a Nikon C1 confocal microscope (Nikon, Tokyo, Japan) under a water-immersed 60× objective (Plan Apo VC) with 561 nm and 637 nm lasers at room temperature (25–30 °C). Cells expressing E3-tagged membrane proteins were labeled with a mixture of donor and acceptor fluorophores (Alexa568 and Alexa647) conjugated with K4 probes in PBS(+) (pH 7.4) for 5 min at room temperature after washing the cells once with PBS(+). The proteins were labeled at various donor mole fractions (X_D) and excited at 561 nm to obtain fluorescence emission spectra from the cell membranes 3 μm above the glass surface. Spectral images in 565–745 nm (resolution: 10 nm) were obtained with a spectrum detector for following analysis of E_{app} values. In the binding assay of K4 probes to the E3 tag fused with EGFR or β_2AR, confocal images were obtained with a standard detector through a BP575 to 615 nm emission filter for the donor and a LP650 nm emission filter for the acceptor.

2.7. Analysis of E_{app} values from observed spectra

We analyzed the oligomeric states of E3-tagged membrane proteins using FRET spectroscopy, as described in a previous study [20]. Briefly, we calculated FRET efficiencies based on sensitized emission of the acceptor fluorophores (Alexa647 or Cy5) from cell membranes. For the deconvolution of the observed spectra into donor and acceptor spectra, we separately obtained the reference spectra of the donor excited at 561 nm and acceptor excited at 637 nm from E3-GpA* (G83I mutant)-CHO (transient). We use the least-squares method to perform deconvolution (see Fig. A4 and ref. 23). Values of the apparent FRET efficiency based on sensitized acceptor emission (E_{app}) were calculated with the equation based on the theory of Meyer *et al.*[26]

$$E_{app} = \frac{\varepsilon_A(\lambda_D^{ex})}{\varepsilon_D(\lambda_D^{ex})} \times \left(\frac{F_{AD} - F_A}{F_A} \right) \quad (1)$$

where $\varepsilon_A(\lambda_D^{ex})$ and $\varepsilon_D(\lambda_D^{ex})$ represent the molar extinction coefficient of the acceptor and donor at 561 nm, respectively, and F_{AD} and F_A indicate the acceptor emission intensity (arbitrary unit) excited at 561 nm in the presence and absence of the donor, respectively. Because F_A could not be directly acquired in the presence of the donor, we also measured the ratio of the fluorescence intensities of the acceptor excited at 561 and 637 nm ($R_{561/637}$) from the E3-GpA mutant (G83I)-CHO (transient) labeled with the acceptor, and then multiplied the fluorescence intensity of the acceptor acquired by the excitation at 637 nm in the presence of the donor by the $R_{561/637}$ ratio to obtain the F_A value.

2.8. Theoretical curves

Taking into account of random labeling of the donor and acceptor in the oligomers, the theoretical curve for E_{app} is given [26], as

$$E_{app} = E \times \frac{X_D}{1-X_D} \times [1-\{X_D(1-X'_U)+X'_U\}^{N-1}] \quad (2)$$

where X_D, X'_U, and N indicate the donor molar fraction over the total (donor and acceptor) molar concentration of the K4 probes, unlabeled receptor fraction, and the number of protomers in an oligomer, respectively. The total molar concentrations of the K4 probes were set such that labeling efficiencies would be approximately 90% (100 nM for E3-EGFR and 50 nM for the other proteins). The X'_U value was estimated to be 0.1 based on the occupancies (~ 90%) of E3-tagged membrane proteins labeled with K4 probes at 50 nM (in the case of E3-β_2AR /GpA*/M2) or 100 nM (E3-EGFR). E represents the true FRET efficiency in the oligomers, which was determined by the distance and mutual orientation of the donor and acceptor. The assumption of a random orientation of the fluorophores was reasonable because of flexible linkers (Gly–Gly–Gly–Ile–Asp) between the E3 tag and N-terminal regions.

2.9. Depletion of sialic acid and cholesterol

After transient transfection, E3-EGFR-expressing CHO-K1 cells were incubated for 2 h in serum-free medium, and then treated with 20 or 100 mU/mL of Arthrobacter ureafaciens neuraminidase (Nacalai Tesque) in serum-free medium for 1 h at 37 °C to deplete sialic acid levels. To metabolically deplete cellular cholesterol, CHO-K1 cells were incubated with 1

μM compactin from seeding to examination, expect for the incubation time, with serum-free medium for 5 h after the transient transfection of EGFR. Other procedures were the same as other FRET experiments.

2.10. Time course of the FRET signal

Time-lapse images were acquired to detect the time course of the EGFR oligomerization induced by the EGF stimulation. After staining cells with Alexa-labeled K4 probes at X_D = 0.5 in 1 mL PBS(+) (pH 7.4) for 5 min at room temperature after washing the cells once with PBS(+), confocal images were obtained under excitation at 561 nm at 25–30 °C. After taking the first three images (4 s intervals), 1 mL of PBS(+) containing the K4 probe (final concentration of 100 nM) and EGF (final concentration of 150 nM) were rapidly mixed with the sample, followed by the taking of images (2 s intervals). The fluorescence spectra from cell membranes at each time point were deconvoluted into donor and acceptor spectra. The ratio of the maximal fluorescence intensity of the acceptor (Em: 665 nm) to donor (Em: 605 nm) (= A/D) was used as a measure of FRET.

3. RESULTS

3.1. EGFR expression and EGF-induced autophosphorylation

Western blot analyses were performed to examine the expression of EGFRs and their phosphorylation activities in CHO-K1 cells. E3-EGFRs were detected as single bands at approximately 175 kDa with both the anti-total EGFR antibody and anti-phosphotyrosine 1173 antibody (see Fig. A1). The intensities of the phosphorylated bands increased with increases in the concentration of EGF. We confirmed that dot blotting gave similar results to Western blotting (see Fig. A1). We performed dot blotting in subsequent experiments to determine the autophosphorylation levels of EGFRs.

3.2. Labeling of EGFRs using the coiled-coil method

CHO-K1 cells expressing E3-fused EGFRs were imaged by confocal microscopy after the specific labeling of cell-surface receptors with K4 probes (Fig. 1). Most receptors remained in the plasma membrane during the observation time (5–25 min after incubation with or without EGF), although EGF-stimulation enhanced internalization (Fig. 1). We analyzed

the fluorescence spectra in the cell membrane region in the following experiments. The K_D values between fluorophore-labeled K4 probes and E3-fused EGFRs (6–8 nM) were similar to those for other E3-tagged membrane proteins used in previous studies (~ 5 nM) (see Fig. A2). To confirm that the E3–K4 complex did not affect EGFR activation, we examined EGF-induced EGFR autophosphorylation with and without K4 probes by immunoblotting. No significant difference was observed with the addition of K4 probes (see Fig. A3).

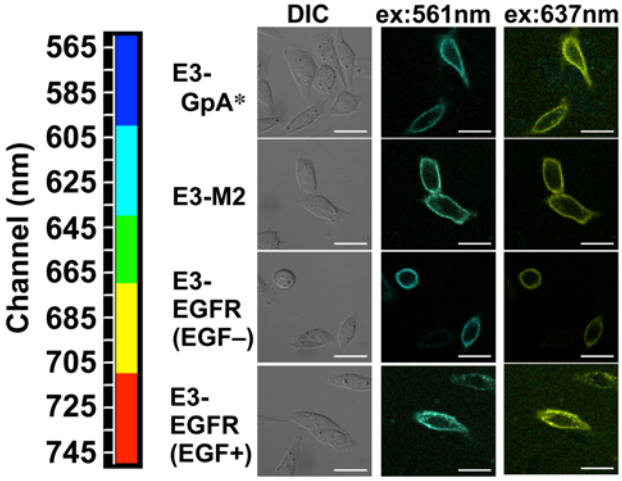

Figure 1. Confocal images of E3-tagged proteins. Representative spectral images are shown in a pseudocolor. E3-tagged proteins were transiently expressed and labeled with a 1:1 mixture of a donor (Alexa568-K4) and acceptor (Alexa647-K4) ($X_D = 0.5$) in PBS (+) (pH 7.4). The total K4 probe concentration was 100 nM (EGFRs) or 50 nM (the other proteins). All images were captured 5–25 min after labeling. GpA* as a standard of a monomer is the G83I mutant of glycophorin A, which was derived from human erythrocytes. M2 as a standard of a dimer is the M2 proton channel derived from influenza A virus. Rat EGFRs were stimulated with 150 nM of rat EGF. Scale bar = 20 μm

3.3. Analysis of oligomeric states

To detect FRET induced by receptor oligomerization, we co-labeled E3-fused proteins on the cell surface with a pair of fluorophores with a large critical distance transfer (Alexa568 and Alexa647, R_0 = 82 Å) at various donor mole fractions (X_D). After the acquisition of spectral images by confocal microscopy, fluorescent spectra from the cell membranes (Fig, 2A) were used to calculate the apparent FRET efficiency (E_{app}) (Eq. 1). A monomeric standard E3-GpA* (G83I mutant) showed E_{app} values of nearly zero independent of X_D, which was consistent with monomers (Fig. 2B). We used the E3-M2 proton channel

derived from influenza A virus as a dimer standard because we recently found that E3-M2 formed dimers at pH 7.4 [27]. These proteins were always used as monomer and dimer standards to confirm the reliability of the E_{app} values of E3-EGFR. We could determine E_{app} values with an accuracy of ± 0.1 [20]. In the FRET analysis, we selected cells expressing a physiological level of EGFRs (5×10^4–2×10^5 receptors/cell) by comparing fluorescence intensities with those for reference cells stably expressing E3-β_2AR (1.3×10^5 receptors/cell) [20] (see Fig. A5). E_{app} values for E3-EGFR were 0.1 or lower in the absence of EGF (Fig. 2C). On the other hand, in the presence of a saturating amount of EGF (150 nM), E_{app} values increased linearly in a X_D-dependent manner with a slope of 0.55 ± 0.03, which was lower than the theoretical value for the dimer with E = 1 (0.9). The FRET signals already reached plateau 2 min after stimulation (see Fig. 4) and did not change significantly 5–25 min after the EGF stimulation (data not shown). Partial dimerization (coexistence of monomers and dimers) and/or a larger donor–acceptor separation in the dimer than the R_0 value of 82 Å (E < 1) may decrease the E_{app} value of stimulated EGFRs. To clarify the contributions of these two possibilities, we performed FRET experiments using another pair of fluorophores (TMR–Cy5), whose R_0 value (53 Å) [28] was shorter than that of the Alexa pair. In this case, the slope of E_{app} was 0.25 ± 0.01 (Fig. 2D). Because of a theoretically linear relationship between E_{app} and X_D, in the case of monomer–dimer transition, an observed value of E_{app} is proportional to a dimer fraction at each X_D. The donor–acceptor distance (R) and corrected dimer fraction of EGFRs (f) were estimated by solving simultaneous equations for the Alexa and TMR–Cy5 pairs as below.

$$Slope = fE(1 - X'_U) = f\left(\frac{0.9}{1 + \left(\frac{R}{R_0}\right)^6}\right) \quad (3)$$

We obtained R and f values of 56 Å and 0.67, respectively. The value of R was plausible for a model that two K4 probes were tethered by the coiled-coil labeling and freely moved around the N termini of the EGFR back-to-back dimer, as determined by X-ray crystallography (~50 Å) [9]. One third of the EGFRs existed as monomers, even in the presence of sufficient EGF ligands. Note that the FRET results do not exclude the possibility of local concentration (clustering) of the receptors into membrane domains without close contacts of the receptors (E = 0).

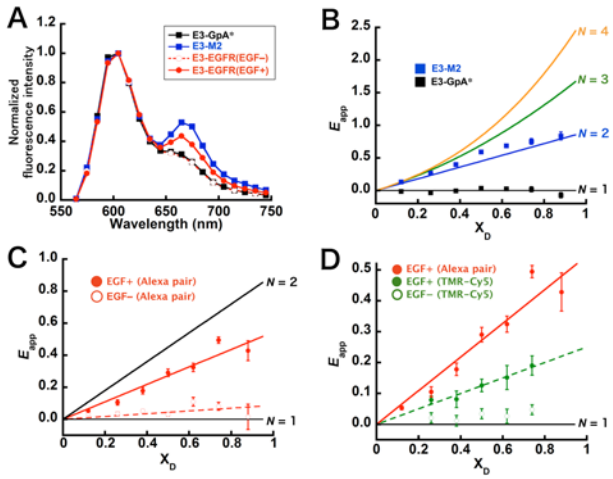

Figure 2. Detection of the oligomeric states of membrane proteins by FRET. (*A*) Fluorescence spectra (Ex : 561 nm) from cell membranes labeled with the Alexa-pair (X_D = 0.5). Fluorescence spectra from at least 10 cells were averaged and normalized at 605 nm. Labeling conditions were the same as those described in Fig. 1. The symbols indicate a GpA G83I mutant (*black squares*), M2 proton channel (*blue squares*), EGFR without EGF (*red open circles*), and EGFR with 150 nM EGF (*red solid circles*). (*B*) Theoretical curves and measured E_{app} values at various donor mole fractions (X_D) using K4 probes labeled with the Alexa pair. Black, blue, green, and yellow lines show theoretical curves for monomers, dimers, trimers and tetramers, respectively. *N* indicates the number of protomers in an oligomer. Black and blue squares indicate the E_{app} values for GpA* and M2, respectively (n > 10). (*C*) The E_{app} values for EGFR with or without 150 nM EGF using K4 probes labeled with the Alexa pair. Open and solid circles indicate values in the absence and presence of EGF, respectively (n > 10). The plots were linearly fit to obtain the slopes. (*D*) Comparison of E_{app} values for EGFR labeled with the Alexa pair (*red*) and the TMR–Cy5 pair (*green*). Open and solid symbols indicate values in the absence and presence of EGF, respectively (n > 10).

3.4. Effects of membrane components on EGFR dimerization

Membrane components such as cholesterol and ganglioside GM3 have been considered as functional modulators for EGFRs and other tyrosine-kinase receptors [29,30]. We examined the relationship between EGFR dimerization and the presence of cholesterol or GM3 by measuring E_{app} values at X_D = 0.74 after the treatment with the lipid-disrupting

reagents. The compactin-induced depletion of cholesterol had no significant effect on the E_{app} value in the presence of EGF (Fig. 3). Similarly, the degradation of GM3 by the treatment with up to 100 mU/mL neuraminidase did not significantly affect the E_{app} value with 150 nM EGF (Fig. 3).

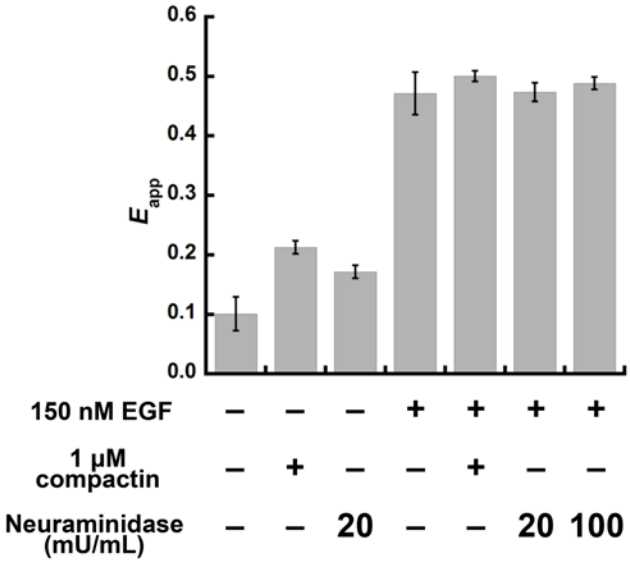

Figure 3. E_{app} values after the depletion of cholesterol or monosialoganglioside GM3. All experiments were performed at X_D = 0.74. Fluorescence spectra from EGF-stimulated CHO-K1 cells were observed 5–25 min after the EGF stimulation. Each value indicates the mean ± SE. (n > 10).

3.5. Time course of EGFR oligomerization and phosphorylation

We detected rapid receptor oligomerization following ligand stimulation with the acceptor/donor fluorescence intensity ratio (A/D). Upon adding EGF to cells, the A/D value increased from the baseline (~ 0.08) to a plateau (~ 0.14) values within 20 s (Fig. 4). The ratio did not change for at least 3 min after reaching the plateau. On the other hand, the EGFR phosphorylation level, examined by dot blotting, exhibited a slower increase than the FRET signal, and reached a plateau at approximately 90 s (Fig. 4). Note that the ligand-independent basal phosphorylation of EGFR in the absence of EGF exhibited the non-zero value (0.2–0.4) (Fig. 4 and Fig. 5A) supposedly due to cells overexpressing receptors, which were excluded in the confocal microscopy-based analyses, whereas ligand-induced phosphorylation should represent the response from cells expressing physiological amount of receptors.

3.6. Dose-response curves

Finally, we examined the EGF concentration-dependence of EGFR dimerization at X_D = 0.74. We determined E_{app} values of EGFRs after 5–25 min stimulation with different concentrations of EGF in the presence of the Alexa K4 probes pair. Percentages of EGFR dimers (dimer fraction at each EGF concentration (f) × 100) were calculated as

$$f \times 100 = \frac{E_{app,\,obs}}{E_{app,\,dimer}} \times 100 = \frac{E_{app,\,obs} \times 100}{E \times \frac{X_D}{1-X_D} \times [1-\{X_D(1-X'_U)+X'_U\}]} = 165.38 \times E_{app,\,obs} \qquad (4)$$

Where $E_{app,obs}$ is an observed value of E_{app}, $E_{app,dimer}$ is the theoretical value of E_{app} considering all EGFRs form dimers. E (= 1 / (1 + $(R/R_0)^6$) is the true FRET efficiency in the dimer considering R = 56 Å and R_0 = 82 Å. X_D and X'_U were fixed at 0.74 and 0.1, respectively. The dimerization of EGFRs significantly increased in an EGF concentration range between 1 nM and 10 nM (an apparent 50% effective dose was ~ 1 nM) (Fig. 5A). At higher concentrations of EGF (> 10 nM), the fraction of dimerized EGFRs was approximately 67% (55–75%). On the other hand, an apparent 50% effective dose of EGFR phosphorylation determined by immunoblotting was ~ 8 nM (Fig. 5A).

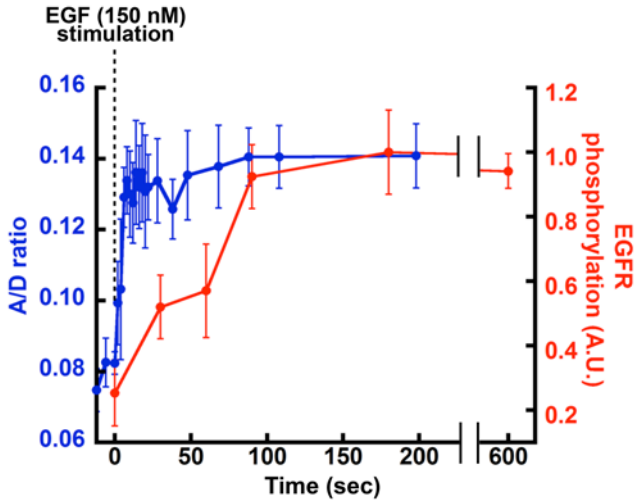

Figure 4. Time courses of dimerization and phosphorylation upon stimulation. A/D is the ratio of the maximal fluorescence intensities of the acceptor (665 nm) to the donor (605 nm), which were obtained from the deconvoluted fluorescence spectra (Ex : 561nm) of four cell membranes. Labeling was performed at X_D = 0.5. The phosphorylation level was the

relative chemiluminescence intensity for phosphorylated Tyr1173 to total EGFR as determined by dot blotting after the stimulation was stopped at each time point by the addition of the lyse buffer. The phosphorylation level was an average from three separately performed experiments. Each value indicates the mean ± SE. ($n > 3$).

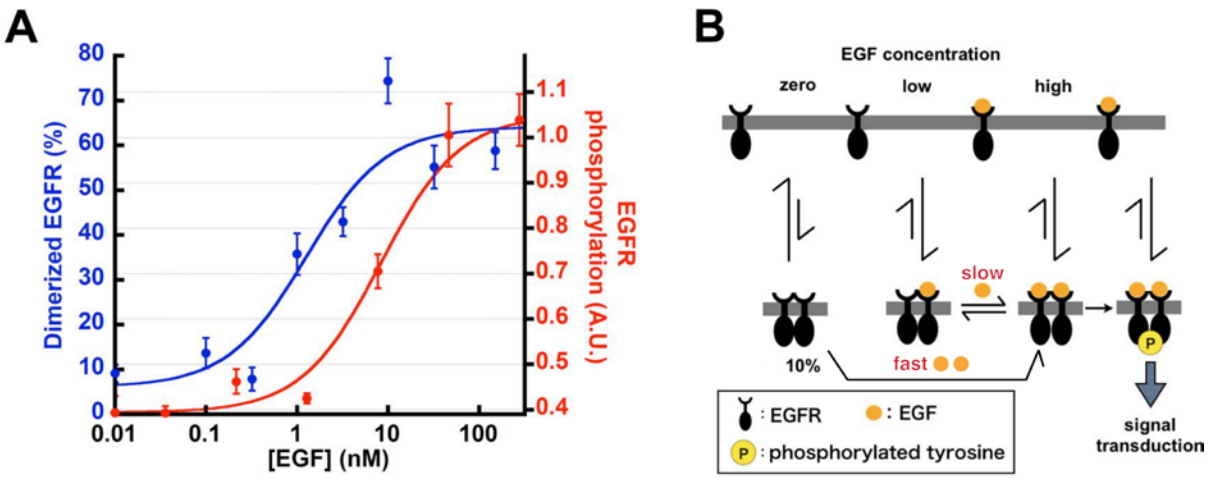

Figure 5. EGF dose-dependent dimerization and phosphorylation of EGFRs. (*A*) The EGF concentration dependencies of EGFRs. Blue: Oligomerization 5–25 min after EGF stimulation. Red: Phosphorylation 5 min after EGF stimulation of EGFRs. The phosphorylation level was obtained from dot blotting (see fig A1, *B*). The dimer fraction was calculated from E_{app} values at $X_D = 0.74$, assuming $R = 56$ Å. Each value indicates the mean ± SE. ($n > 10$). (*B*) Proposed model for the activation of EGFRs induced by EGF.

4. DISCUSSION

4.1. Oligomeric states of EGFRs

The mechanism underlying EGFR oligomerization is not simple because the strength of ligand affinity and receptor self-association are intricately related to each other. For example, negative cooperativity has been reported for the ligand binding of EGFRs [11–13], which indicates that EGFRs have two distinguishable binding sites to their ligand and binding of the ligand to the first site reduces affinity for the second site [13]. Moreover, the degree of oligomerization generally depends on the expression level according to the association constants [13]. Under our experimental conditions (5×10^4–2×10^5 receptors/cell), EGFRs appeared to exist as monomers or dimers without forming higher-order oligomers, because the E_{app} plot of EGFR with 150 nM EGF gave the best fit with a linear shape (fig. 2C and D),

which is characteristic of the dimer. On the other hand, downward-convex curves are characteristic of the trimer or higher oligomers (fig. 2B). The majority of EGFRs could be regarded as monomers in the resting state (~ 90%) with a small fraction of predimers (~10%), whereas ~70% of the EGFRs formed dimers after ligand stimulation. The observed degrees of oligomerization appear to be lower than those in previous reports describing significant formation of predimers and higher-order oligomers in the absence of EGF [31,32]. The host cell line and the expression level can significantly affect the oligomeric and clustering states of the receptors. Clayton and coworkers reported tetramers (or higher order oligomers) of unligated EGFR in epidermoid carcinoma A431 cells [31]. On the other hand, Saffarian et al. reported ~70% monomeric EGFRs in the resting state in CHO cells [32]. In our experiments, the coiled-coil labeling may slightly interfere the oligomerization to underestimate the oligomer population, although the N-termini were separated in the dimer (~56 Å, estimated from Equation 3), and the K4 labeling did not affect the phosphorylation of the receptors (Fig. A3).

4.2. Factors affecting EGFR dimerization

The monomer–dimer transition of EGFRs may be regulated by several factors other than the receptor concentration. One possible reason why not all EGFRs formed dimers following the EGF stimulation is the interaction between plasma membrane components and EGFRs. Cholesterol and GM3 have been shown to interact with EGFRs, thereby diminishing ligand-induced EGFR phosphorylation, whereas the removal of cholesterol from cell membranes or degradation of GM3 increased EGFR phosphorylation [29,30]. Therefore, it is plausible to assume that these lipids suppress receptor oligomerization. However, we observed no significant effect of the depletion of cholesterol or GM3 on the oligomeric states of EGFRs in the presence of 150 nM EGF (Fig. 3). These results suggest that cholesterol and GM3 had no effect on EGFR dimerization in ligand-occupied extended EGFRs. These results indicate that these two membrane components inhibit EGFR phosphorylation by different mechanisms from the regulation of oligomeric states. Other factors may explain the co-existence of EGFR monomers and dimers after the ligand stimulation. The extracellular domain of EGFRs may remain a steric hindrance to dimerization to some extent. A previous study reported that an EGFR mutant lacking much of the EGFR extracellular domain exhibited stronger phosphorylation activity than that of the wild-type regardless of the ligand stimulation [33]. Furthermore, the cationic residues of the kinase domain may interact with anionic lipids (e.g., phosphatidylserine) on the inner leaflet to hinder EGFR

dimerization, although the intracellular domains of EGFRs also exhibit dimerizing abilities [7]. EGFR phosphorylation can also enhance the dissociation of dimers into monomers [13,34]. In the present study, the fluorescence spectra acquired from the cell membrane contained temporally averaged information regarding the EGFR oligomeric state. Therefore, it remains unclear whether the coexistence of monomers and dimers reflects two static species or a dynamic equilibrium between them. Single molecule studies reported that dimers were not very stable (lifetimes in the order of seconds), even in the ligand-bound form [35]. Therefore, at least some of the EGF-resistant monomers observed should be in dynamic equilibrium with dimers.

4.3. Relationship between EGFR dimerization and phosphorylation

As far as we know, it is the first time to investigate quantitatively the relationship of time-courses of the EGFR dimerization and autophosphorylation induced by EGF stimulation. The receptors rapidly oligomerized within 20 s after EGF stimulation (Fig. 4). EGF association rate was estimated by using reported rate constants for high-affinity and low affinity sites [36,37]. In our condition of 150 nM EGF, the observed oligomerization rate (k ~ 0.1 sec^{-1}, Figure 4) was comparable or lower than the binding rates for both high-affinity (k_{high} = 0.23–60 sec^{-1}) and low-affinity (k_{low} = 0.084–0.6 sec^{-1}) sites, although the formation of low-affinity inactive dimer may prevent complete ligand binding to all receptors (see below). The theoretical random collision rate of EGFR monomers is sufficiently fast (k = 5.6 sec^{-1}) and can explain the quick dimerization under the experimental conditions (calculated according to Eq. 13b of reference [38], assuming receptors per cell of 50,000 with a cell diameter of 20 μm, critical collision distance of 1 nm, and a diffusion coefficient [35] of 0.05 μm^2 sec^{-1}). The delayed EGFR phosphorylation upon ligand binding revealed that EGFR dimerization preceded its phosphorylation (Fig. 4). This finding is consistent with the conventional view that EGFR autophosphorylation requires the formation of the asymmetric kinase domain dimers [7]. Moreover, as shown in Fig. 5A, the dose-response of EGFR dimerization shifted to the left of the phosphorylation curve. Considering that a subnanomoler range of EGF can trigger significant signaling by binding to the high-affinity site [37,46], the saturation of phosphorylation should require sufficient EGF binding to the low-affinity site, although it may not be related to signaling in physiological conditions. The apparent 50% effective doses of EGFR dimerization and phosphorylation were approximately 1 nM and 8 nM, respectively, with the former being within the reported apparent binding affinities (K_D) of EGFR to its ligand (0.27–5 nM [39–43]). The latter

less-sensitive phosphorylation activities have also been reported in literatures [44,45]. These results confirm that the N-terminal coiled-coil labeling did not significantly affect the receptor function. EGFRs were significantly dimerized while maintaining the basal phosphorylation level especially at 1 nM of EGF. A formation of kinase-inactive dimers may explain the experimental observation. A possible model for this inactive dimer is an EGFR dimer that binds to a single EGF, which can be activated by the binding of a second ligand (Fig. 5B). A ligand-occupied EGFR monomer was more likely to encounter an unoccupied monomer at EGF concentrations of 1–10 nM, and they could form an inactive dimer with a single ligand. This observation is consistent with negative cooperativity for the ligand binding to EGFRs [11–13]. On the other hand, other studies have shown that low receptor occupancy is sufficient to trigger signaling, suggesting that EGF binding to high affinity receptors has positive cooperativity [36,37,46]. We propose a hypothetical model to explain these observations. In this model, binding of an EGF to the predimer (~10% in this study) accelerates binding of the second EGF and rapid activation (high-affinity dimer with positive cooperativity) [36], whereas association of EGF-bound monomer to unbound monomer decelerates the binding of the second ligand (ligand-induced low-affinity dimer with negative cooperativity) (Fig. 5B). In previous models, these single-liganded dimers are not discriminated as different species [5,12,36,47]. The interconversion between these species may be slowed down due to steric hindrance in the dimers. Liu *et al.* showed that EGFR dimers occupied with a single EGF can be phosphorylated by means of cotransfection of two kinds of EGFR mutants that lack the ligand-binding or kinase activity, respectively [48], but they did not examine the ratio of phosphorylated single-occupied dimers over all dimers in the experimental condition. Moreover, a phosphorylation level of the single-occupied dimer mutants was significantly lower than that of dimers of intact EGFRs in the presence of EGF. It is also unclear whether the difference of phosphorylation levels between the single-occupied dimer mutants in the presence and absence of EGF was significant or not in this report [48]. Considering the Liu's report, the single-occupied dimers may have partial phosphorylation activity, however the main source of EGFR phosphorylation was the double occupied dimers at least in the presence of 1 nM or higher concentrations of EGF in our experimental conditions.

5. Conclusion

We succeeded in elucidating the oligomeric states of EGFRs on living CHO cell membranes using a combination of the coiled-coil method and FRET analysis based on confocal spectral

microscopy. Comparing with other previous reports on EGFR activities we emphasize that this approach is quantitative and enables time-resolved analysis for living cells. Our results showed that the majority of EGFRs assumed a monomer form in the absence of their ligands with a small fraction of predimer (~10%). The ligand stimulation led to ~60% of EGFRs altering their oligomeric state from monomers to dimers, while the remaining receptors existed as monomers. The formation of dimers by the ligand stimulation preceded its phosphorylation in both time and ligand-dose dependent manners. These results indicate that the formation of EGFR dimers induced by the ligand stimulation plays a major role in EGFR autophosphorylation. Regarding the clinical importance of EGFRs, several kinds of cancerous cells overexpress EGFRs (e.g., A431 cells ($> 2 \times 10^6$ receptors/cell) [49]) or have pathogenic EGFR mutations [50]. The method used in this study could reveal the behavior of EGFRs in the context of these malignant cells. Moreover, the coiled-coil labeling method could be applicable to other ErbB family receptors and other membrane proteins, so this approach could help to understand comprehensively the interactions of EGFRs and other related membrane proteins with high quantitative accuracy in the future.

Acknowledgement

This work was financially supported in part by JSPS KAKENHI Grant Numbers 21390007 and 24390009, Japan and by a grant from Takeda Science Foundation.

Appendix A. Supplementary information

DNA oligonucleotide sequences for the construction of E3-ratEGFR-pcDNA3 (Table A1), immunoblotting of EGFR (Fig. A1), binding assay for K4 probes (Fig. A2), EGFR autophosphorylation activity with/without a K4 probe (Fig. A3), deconvolution of observed spectra from the membrane with K4 probes at $X_D = 0.5$ (Fig. A4), expression level of E3-fused proteins on the plasma membrane (Fig. A5) are available at http://

References

[1] K. Sakaguchi, Y. Okabayashi, Y. Kido, S. Kimura, Y. Matsumura, K. Inushima, M. Kasuga, Shc phosphotyrosine-binding domain dominantly interacts with epidermal growth factor receptors and mediates Ras activation in intact cells, Mol Endocrinol, 12 (1998) 536–543.

[2] J. Mendelsohn, J. Baselga, The EGF receptor family as targets for cancer therapy, Oncogene, 19 (2000) 6550–6565.
[3] I. Okamoto, Epidermal growth factor receptor in relation to tumor development: EGFR-targeted anticancer therapy, FEBS J, 277 (2010) 309–315.
[4] W.A. Franklin, R. Veve, F.R. Hirsch, B.A. Helfrich, P.A. Bunn, Jr., Epidermal growth factor receptor family in lung cancer and premalignancy, Semin Oncol, 29 (2002) 3–14.
[5] M.A. Lemmon, Ligand-induced ErbB receptor dimerization, Exp Cell Res, 315 (2009) 638–648.
[6] K.M. Ferguson, Structure-based view of epidermal growth factor receptor regulation, Annu Rev Biophys, 37 (2008) 353–373.
[7] X. Zhang, J. Gureasko, K. Shen, P.A. Cole, J. Kuriyan, An allosteric mechanism for activation of the kinase domain of epidermal growth factor receptor, Cell, 125 (2006) 1137–1149.
[8] K.M. Ferguson, M.B. Berger, J.M. Mendrola, H.S. Cho, D.J. Leahy, M.A. Lemmon, EGF activates its receptor by removing interactions that autoinhibit ectodomain dimerization, Mol Cell, 11 (2003) 507–517.
[9] H. Ogiso, R. Ishitani, O. Nureki, S. Fukai, M. Yamanaka, J.H. Kim, K. Saito, A. Sakamoto, M. Inoue, M. Shirouzu, S. Yokoyama, Crystal structure of the complex of human epidermal growth factor and receptor extracellular domains, Cell, 110 (2002) 775–787.
[10] T.P. Garrett, N.M. McKern, M. Lou, T.C. Elleman, T.E. Adams, G.O. Lovrecz, H.J. Zhu, F. Walker, M.J. Frenkel, P.A. Hoyne, R.N. Jorissen, E.C. Nice, A.W. Burgess, C.W. Ward, Crystal structure of a truncated epidermal growth factor receptor extracellular domain bound to transforming growth factor alpha, Cell, 110 (2002) 763–773.
[11] R. Zidovetzki, D.A. Johnson, D.J. Arndt-Jovin, T.M. Jovin, Rotational mobility of high-affinity epidermal growth factor receptors on the surface of living A431 cells, Biochemistry, 30 (1991) 6162–6166.
[12] C. Wofsy, B. Goldstein, K. Lund, H.S. Wiley, Implications of epidermal growth factor (EGF) induced egf receptor aggregation, Biophys J, 63 (1992) 98–110.
[13] L.J. Pike, Negative co-operativity in the EGF receptor, Biochem Soc Trans, 40 (2012) 15–19.
[14] T. Moriki, H. Maruyama, I.N. Maruyama, Activation of preformed EGF receptor dimers by ligand-induced rotation of the transmembrane domain, J Mol

Biol, 311 (2001) 1011–1026.
[15] A.H. Clayton, F. Walker, S.G. Orchard, C. Henderson, D. Fuchs, J. Rothacker, E.C. Nice, A.W. Burgess, Ligand-induced dimer-tetramer transition during the activation of the cell surface epidermal growth factor receptor-A multidimensional microscopy analysis, J Biol Chem, 280 (2005) 30392–30399.
[16] E.G. Hofman, A.N. Bader, J. Voortman, D.J. van den Heuvel, S. Sigismund, A.J. Verkleij, H.C. Gerritsen, P.M. van Bergen en Henegouwen, Ligand-induced EGF receptor oligomerization is kinase-dependent and enhances internalization, J Biol Chem, 285 (2010) 39481–39489.
[17] N. Kawashima, K. Nakayama, K. Itoh, T. Itoh, M. Ishikawa, V. Biju, Reversible dimerization of EGFR revealed by single-molecule fluorescence imaging using quantum dots, Chemistry, 16 (2010) 1186–1192.
[18] A. Salahpour, B. Masri, Experimental challenge to a 'rigorous' BRET analysis of GPCR oligomerization, Nat Methods, 4 (2007) 599–600; author reply 601.
[19] Y. Yano, A. Yano, S. Oishi, Y. Sugimoto, G. Tsujimoto, N. Fujii, K. Matsuzaki, Coiled-coil tag–probe system for quick labeling of membrane receptors in living cell, ACS Chem Biol, 3 (2008) 341–345.
[20] K. Kawano, Y. Yano, K. Omae, S. Matsuzaki, K. Matsuzaki, Stoichiometric analysis of oligomerization of membrane proteins on living cells using coiled-coil labeling and spectral imaging, Anal Chem, 85 (2013) 3454–3461.
[21] Y. Yano, K. Matsuzaki, Fluorescence ratiometric detection of ligand-induced receptor internalization using extracellular coiled-coil tag–probe labeling, FEBS Lett, 585 (2011) 2385–2388.
[22] A.W. Krug, C. Schuster, B. Gassner, R. Freudinger, S. Mildenberger, J. Troppmair, M. Gekle, Human epidermal growth factor receptor-1 expression renders Chinese hamster ovary cells sensitive to alternative aldosterone signaling, J Biol Chem, 277 (2002) 45892–45897.
[23] E. Tzahar, H. Waterman, X. Chen, G. Levkowitz, D. Karunagaran, S. Lavi, B.J. Ratzkin, Y. Yarden, A hierarchical network of interreceptor interactions determines signal transduction by Neu differentiation factor/neuregulin and epidermal growth factor, Mol Cell Biol, 16 (1996) 5276–5287.
[24] A.R. Zurita, P.M. Crespo, N.P. Koritschoner, J.L. Daniotti, Membrane distribution of epidermal growth factor receptors in cells expressing different gangliosides, Eur J Biochem, 271 (2004) 2428–2437.
[25] R.H. Tao, I.N. Maruyama, All EGF(ErbB) receptors have preformed homo-

and heterodimeric structures in living cells, J Cell Sci, 121 (2008) 3207–3217.
[26] B.H. Meyer, J.M. Segura, K.L. Martinez, R. Hovius, N. George, K. Johnsson, H. Vogel, FRET imaging reveals that functional neurokinin-1 receptors are monomeric and reside in membrane microdomains of live cells, Proc Natl Acad Sci U S A, 103 (2006) 2138–2143.
[27] K. Kawano, Y. Yano, K. Matsuzaki, A dimer is the minimal proton-conducting unit of the influenza a virus m2 channel, J Mol Biol, 426 (2014) 2679–2691.
[28] T. Ha, A.Y. Ting, J. Liang, W.B. Caldwell, A.A. Deniz, D.S. Chemla, P.G. Schultz, S. Weiss, Single-molecule fluorescence spectroscopy of enzyme conformational dynamics and cleavage mechanism, Proc Natl Acad Sci U S A, 96 (1999) 893–898.
[29] L.J. Pike, L. Casey, Cholesterol levels modulate EGF receptor-mediated signaling by altering receptor function and trafficking, Biochemistry, 41 (2002) 10315–10322.
[30] Q. Zhou, S. Hakomori, K. Kitamura, Y. Igarashi, GM3 directly inhibits tyrosine phosphorylation and de-N-acetyl-GM3 directly enhances serine phosphorylation of epidermal growth factor receptor, independently of receptor-receptor interaction, J Biol Chem, 269 (1994) 1959–1965.
[31] A.H.A. Clayton, M.L. Tavarnesi, T.G. Johns, Unligated epidermal growth factor receptor forms higher order oligomers within microclusters on A431 cells that are sensitive to tyrosine kinase inhibitor binding, Biochemistry, 46 (2007) 4589–4597.
[32] S. Saffarian, Y. Li, E.L. Elson, L.J. Pike, Oligomerization of the EGF receptor investigated by live cell fluorescence intensity distribution analysis, Biophys J 93 (2007) 1021–1031.
[33] N.F. Endres, R. Das, A.W. Smith, A. Arkhipov, E. Kovacs, Y. Huang, J.G. Pelton, Y. Shan, D.E. Shaw, D.E. Wemmer, J.T. Groves, J. Kuriyan, Conformational coupling across the plasma membrane in activation of the EGF receptor, Cell, 152 (2013) 543–556.
[34] J.L. Macdonald-Obermann, L.J. Pike, The intracellular juxtamembrane domain of the epidermal growth factor (EGF) receptor is responsible for the allosteric regulation of EGF binding, J Biol Chem, 284 (2009) 13570–13576.
[35] S.T. Low-Nam, K.A. Lidke, P.J. Cutler, R.C. Roovers, P.M. van Bergen en Henegouwen, B.S. Wilson, D.S. Lidke, ErbB1 dimerization is promoted by domain co-confinement and stabilized by ligand binding, Nat Struct Mol Biol, 18 (2011)

1244–1249.
[36] Y. Teramura, J. Ichinose, H. Takagi, K. Nishida, T. Yanagida, Y. Sako, Single-molecule analysis of epidermal growth factor binding on the surface of living cells, EMBO J, 25 (2006) 4215–4222.
[37] H.S. Wiley, B.J. Walsh, K.A. Lund, Global modulation of the epidermal growth factor receptor is triggered by occupancy of only a few receptors, J Biol Chem, 264 (1989) 18912–18920.
[38] O.G. Berg, P.H. von Hippel, Diffusion-controlled macromolecular interactions, Ann Rev Biophys Biophys Chem, 14 (1985) 131–160.
[39] M. Korc, L.M. Matrisian, S.R. Planck, B.E. Magun, Binding of epidermal growth factor in rat pancreatic acini, Biochem Biophys Res Commun, 111 (1983) 1066–1073.
[40] K.W. Ng, N.C. Partridge, M. Niall, T.J. Martin, Epidermal growth factor receptors in clonal lines of a rat osteogenic sarcoma and in osteoblast-rich rat bone cells, Calcif Tissue Int, 35 (1983) 298–303.
[41] P.B. Jones, T.H. Welsh, Jr., A.J. Hsueh, Regulation of ovarian progestin production by epidermal growth factor in cultured rat granulosa cells, J Biol Chem, 257 (1982) 11268–11273.
[42] L. Raaberg, E. Nexo, S. Buckley, W. Luo, M.L. Snead, D. Warburton, Epidermal growth factor transcription, translation, and signal transduction by rat type II pneumocytes in culture, Am J Respir Cell Mol Biol, 6 (1992) 44–49.
[43] N. Matsuda, N.M. Kumar, P.R. Ramakrishnan, W.L. Lin, R.J. Genco, M.I. Cho, Evidence for up-regulation of epidermal growth-factor receptors on rat periodontal ligament fibroblastic cells associated with stabilization of phenotype in vitro, Arch Oral Biol, 38 (1993) 559–569.
[44] B.N. Kholodenko, O.V. Demin, M. Gisela, J.B. Hoek, Quantification of short term singnaling by the epidermal growth factor receptor, J Biol Chem, 274 (1999) 30169–30181.
[45] P.J. Bertics, W.S. Chen, L. Hubler, C. Lazar, M.G. Rosenfeld, G. N. Gill, Alteration of epidermal growth factor receptor activity by mutation of its primary carboxy-terminal site of tyrosine self-phosphorylation, J Biol Chem, 263 (1988) 3610–3617.
[46] P.J. Verveer, F.S. Wouters, A.R. Reynolds, P.H.I.Bastians, Quantitative imaging of lateral ErbB1 receptor signal propagation in the plasma membrane, Science, 290 (2000) 1567–1570.

[47] N.J. Bessman, D.M. Freed, M.A. Lemmon, Putting together structures of epidermal growth factor reeptors, Curr Opin Struc Biol, 29 (2014) 95–101.
[48] P. Liu, T.E. Cleveland 4th, S. Bouyain, P.O. Byrne, P.A. Longo, D.J. Leahy, A single ligand is sufficient to activate EGFR dimers, Proc Natl Acad Sci U S A, 109 (2012) 10861–10866.
[49] H. Haigler, J.F. Ash, S.J. Singer, S. Cohen, Visualization by fluorescence of the binding and internalization of epidermal growth factor in human carcinoma cells A-431, Proc Natl Acad Sci U S A, 75 (1978) 3317–3321.
[50] C.T. Kuan, C.J. Wikstrand, D.D. Bigner, EGF mutant receptor vIII as a molecular target in cancer therapy, Endocr Relat Cancer, 8 (2001) 83–96.

Supplementary information for Oligomeric states of EGFR detected on living cells by the coiled-coil labeling and FRET microscopy

Hirotaka Yamashita[1], Yoshiaki Yano[1], Kenichi Kawano[1], and Katsumi Matsuzaki[1,2]

Supplementary Table

Table A1. List of DNA oligonucleotide sequence for the construction of E3-ratEGFR-pcDNA3
Bold capital letters show restriction enzyme sites. Under lines show protein coding regions.

DNA name	Sequence (5'-3')
Fwd-sig	tt**GAATTC**cccacc<u>atgctgcgaggccagcggcac</u> EcoR**I** rat TrkA signal sequence
Rev-sig	cctaag**CTCGAG**<u>ggatgcggcgcaagcacaagcc</u> Xho**I** rat TrkA signal sequence
Fwd-E3 tag	**CTCGAG**<u>gaaatcgccgctctggaaaaagagatcgctgctctggagaaggagattgccgcccttgagaagggcggcggc</u>**ATCGAT**t Xho**I** E3 tag Cla**I**
Rev-E3 tag	ctaga**ATCGAT**<u>gccgccgccttctcaagggcggcaatctccttctccagagcagcgatctcttttccagagcggcgatttcc</u> Cla**I** E3 tag
Fwd-EGFR	gt**ATCGAT**<u>ctggaggaaaagaaagtttgccaagg</u> Cla**I** EGFR
Rev-EGFR	at**GCTAGC**<u>tcatgctccactaaactcactgcttg</u> Nhe**I** EGFR
Fwd-RE	**CGAT**tccgga**GCTAGC**accggtgcggccgcgatatcgttaact Cla**I** Nhe**I**
Rev-RE	**CTAGA**gttaacgatatcgcggccgcaccggt**GCTAGC**tccggaat Xba**I** Nhe**I**

[1]Graduate School of Pharmaceutical Sciences, Kyoto University, Sakyo-ku, Kyoto 606-8501, Japan
[2]Corresponding author.

Supplementary Methods

Construction of a Plasmid Containing E3-ratEGFR-pcDNA3

All DNA primers used are listed in table S1. Total RNA from PC12 cells was purified using the RNeasy Mini Kit (Qiagen, Maryland, USA). The cDNA encoding kozak sequence, followed by the rat TrkA signal sequence were obtained from total RNA using RT-PCR with primers (Fwd-sig and Rev-sig). The cDNA encoding rat EGFR (NCBI Reference Sequence: NM_031507.1) from the rat brain was also obtained using Fwd-EGFR and Rev-EGFR. The Fwd-E3 tag and Rev-E3 tag were annealed to each other and ligated into the Xho I –Xba I site of pcDNA3, and Fwd-RE and Rev-RE were then annealed and ligated into the Cla I –Xba I site located downstream of the E3 tag sequence. The cDNA encoding rat TrkA signal sequence was ligated into the EcoR I –Xho I site located upstream of the E3 tag sequence. The cDNA encoding rat EGFR was ligated into the Cla I –Nhe I site located downstream of the E3 tag sequence. Sequence of the final product was verified using a DNA sequencer.

Effects of the K4 Probe on EGFR Autophosphorylation

E3-EGFR-expressing cells were prepared as described in the Materials and Methods. After 3h of serum starvation, cells were incubated with 0.5 mL of PBS containing 0 or 100 nM Alexa568-K4 for 5 minutes. A total of 0.5 mL of PBS containing 0 or 150 nM EGF and 0 or 100 nM Alexa568-K4 was then added into cells for 5 minutes at room temperature. After removing PBS, the cells were lysed and used for immunoblotting as described in the Materials and Methods.

Binding Assay for K4 Probes

CHO cells expressing E3-β_2AR (stable) or E3-EGFR-CHO (transient) were placed in a 35-mm glass bottom dish. The cells were labeled with a K4 probe at concentrations of 2.5, 10, 20, 50, and 100 nM. After a 5 min incubation at room temperature, confocal images were acquired using the Nikon C1 confocal microscope to obtain the fluorescence intensity of the cell surface. K_D values of K4 probes and the occupancies of E3-tagged receptors labeled with K4 probes were determined as

$$[R] = [R]_{total} \times \frac{[R]_{free}}{[R]_{free} + K_D} \quad \text{(S1)}$$

where $[R]$ denotes the amount of K4 probe-bound E3-receptors, $[R]_{total}$ indicates the amount of total E3-fused proteins on the cell surface and was equal to maximal binding, which was

approached asymptotically in the saturation curves, $[P]_{free}$ is the free concentration of K4 probes, and K_D is the dissociation constant. In order to correct the EGFR expression level of each cell, fluorescence intensities after labeling with 100 nM of the K4 probe were also acquired from the same cell after noting each concentration of the K4 probes.

Supplementary Figures

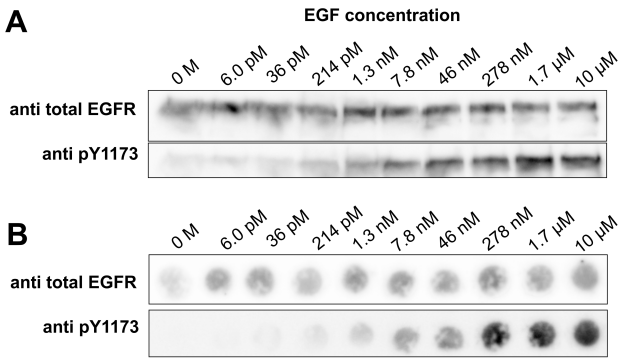

Figure A1. Western blotting (*A*) and dot blotting (*B*) of EGFR

Chemiluminescence detected by the anti-total EGFR antibody (sc-373746) or anti-phosphotyrosine 1173 antibody (sc-101668). Before lysing, samples were incubated with each concentration of EGF indicated above for 5 min.

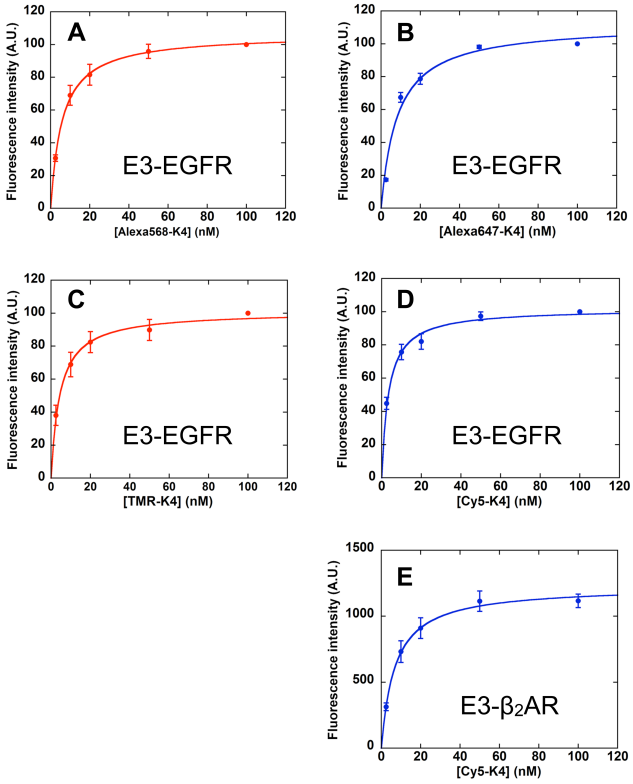

Figure A2. Binding assay for the K4 probes

Fluorescence intensities obtained from the plasma membranes were plotted as a function of K4 probe concentrations. Solid curves show a fit with eq. S1. Error bars indicate the standard errors. In the case of E3-EGFR, fluorescence intensities were normalized by the EGFR expression level on each cell membrane. (*A*) Binding curve for E3-EGFR and Alexa568-K4. K_D = 5.8 ± 0.3 nM (n = 4). (*B*) Binding curve for E3-EGFR and Alexa647-K4. K_D = 8.3 ± 2.0 nM (n = 4). (*C*) Binding curve for E3-EGFR and TMR-K4. K_D = 4.4 ± 0.5 nM (n = 6). (*D*) Binding curve for E3-EGFR and Cy5-K4. K_D = 3.4 ± 0.5 nM (n = 6). (*E*) Binding curve for E3-β_2AR and Cy5-K4. K_D = 6.9 ± 0.7 nM (n = 10).

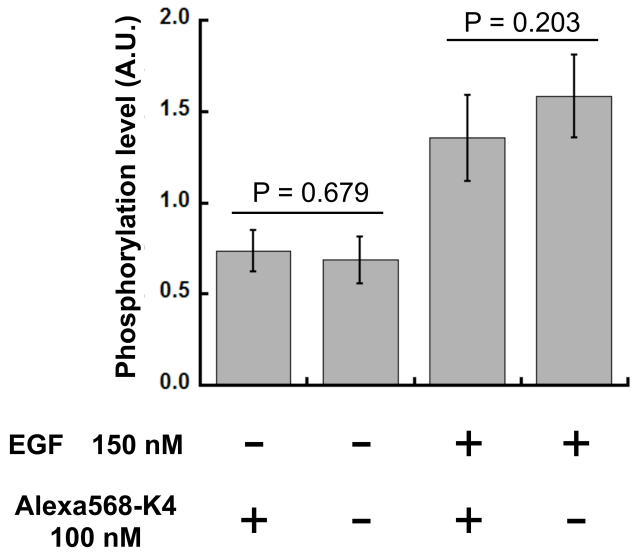

Figure A3. EGFR autophosphorylation activity with/without a K4 probe. Error bars indicate the standard deviation (n = 3). P indicates P values from two-tailed Student's t tests.

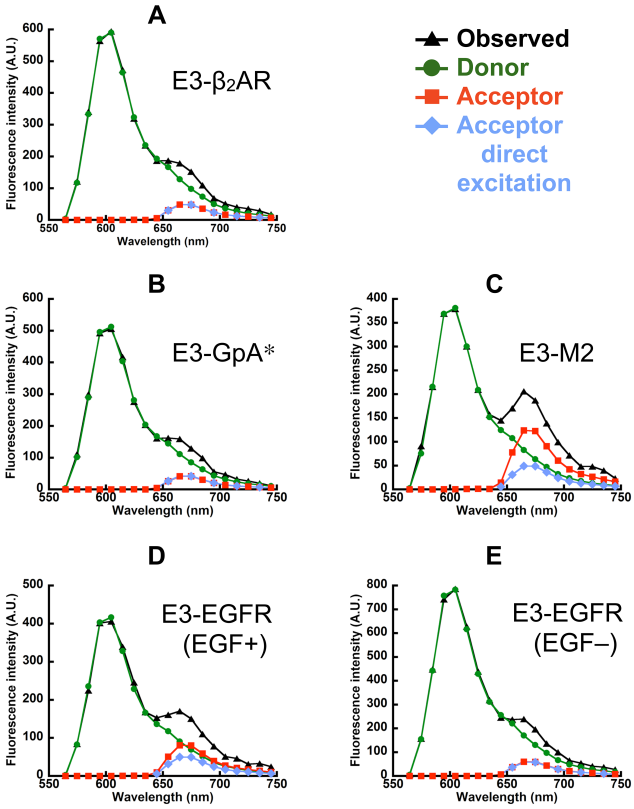

Figure A4. Deconvolution of observed spectra from the membrane with K4 probes at X_D = 0.5

Representative spectra for (*A*) E3-β2AR-CHO (stable), (*B*) E3-GpA*-CHO (transient), (*C*) E3-M2-CHO (transient), and E3-EGFR-CHO (transient) with (*D*) or without (*E*) 150 nM EGF, respectively. Black, green, red, and blue lines show the observed spectra, the deconvoluted spectral components of the donor, that of the acceptor, and the spectra expected for directly excited acceptors at 561 nm, respectively.

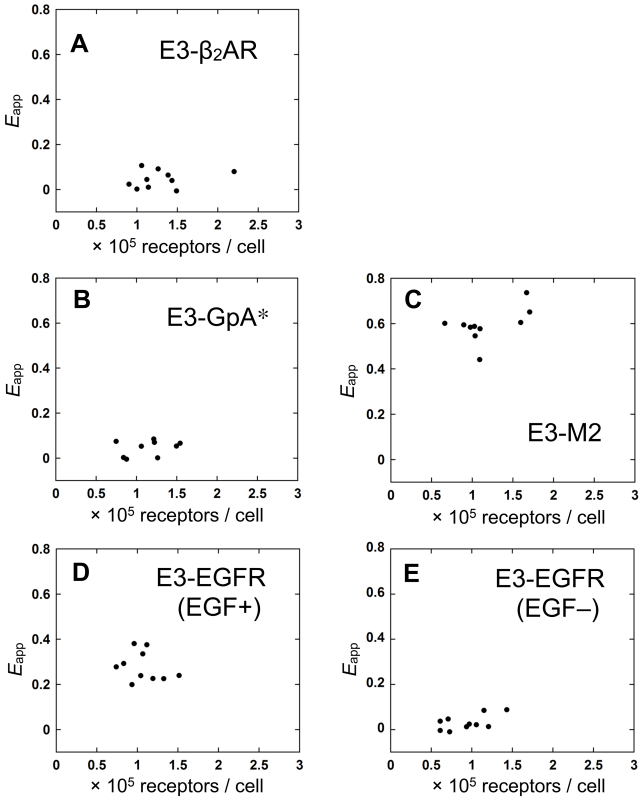

Figure A5. Effects of the expression levels of E3-fused proteins on E_{app} values

The Y-axis indicates E_{app} at X_D = 0.74. The X-axis denotes the expression levels of E3-tagged proteins calculated from fluorescence intensities (Ex: 647 nm / Em: 665 nm) (The averaged fluorescence intensity from E3-β2AR-CHO was considered to be 1.3×10^5 receptors/cell). E_{app} values were not dependent on expression levels, which were maintained under the physiological levels. (*A*) E3-β2AR-CHO (stable), (*B*) E3-GpA*-CHO (transient), (*C*) E3-M2-CHO (transient), and E3-EGFR-CHO (transient) with (*D*) or without (*E*) 150 nM EGF, respectively (n = 10).